Performances of Conventional SOAs Versus QD-SOA in 1530-nm Upstream Transmission of 40 Gb/s Access Network

Budsara Boriboon, Duang-rudee Worasucheep, Satoshi Shimizu, Satoshi Shinada, Hideaki Furukawa, Atsushi Matsumoto, Kouichi Akahane, Naokatsu Yamamoto, and Naoya Wada

***Abstract*—SOA is the key device for burst-mode upstream transmission of 40 Gb/s access network to extend distance and increase users. We evaluate two conventional SOAs and our QD-SOA in networks, consisting of 20-km Single Mode Fiber (SMF) and splitters (1:8, 1:16 & 1:32). First, their characteristics are reported: 3-dB bandwidth & peak wavelength of Amplified Spontaneous Emission (ASE) spectra, gain, saturation output & input, and Noise Figure (NF). QD-SOA gives the lowest NF of 4.59 dB at –20-dBm input due to its highest Optical Signal to Noise Ratio (OSNR). It also has the fastest response time (70 ps) with less data pattern effect when operating in saturation region. Besides the measurement of Input Power Dynamic Range (IPDR) of 3 SOAs, their performances of single versus two-cascaded SOA transmissions are evaluated by Bit Error Rate (BER) in many combinations of SMF and splitters. In case of inserting 1:8 splitter between two-cascaded SOAs, the performance of 2nd-stage QD-SOA has lower BERs than 2nd-stage conventional SOA due to its higher saturation output and less pattern effect when operating at high input power. Finally, both experimental and computed BERs are plotted versus SOA's input to confirm the OSNR degradation and data pattern effect.**

***Index Terms*—40 Gb/s access network, cascaded SOAs, conventional SOA, data pattern effect, input power dynamic range, NG-PON2, optical signal to noise ratio, QD-SOA.**

I. Introduction

OPTICAL amplifier, such as Erbium-Doped Fiber Amplifier (EDFA) and Semiconductor Optical Amplifier (SOA), can be applied in Passive Optical Network (PON) to extend transmission distance and support many users. The advantages of SOA over EDFA are lower cost, less power consumption, more compact size, and simpler integration with other components and electronic boards. Plus, it can amplify any wavelength range depending on doped elements. For example, the combination of InGaAsP as well as InGaAlAs can amplify all wavelengths across both O-band (1300 nm) and C-band (1550 nm). To improve characteristics of SOA, the Quantum Dot SOA (QD-SOA) has been developed with superior properties, e.g., low Noise Figure (NF), less chirp, fast response time, and less pattern effect [1]. The faster response of QD-SOA is beneficial to many applications, such as all-optical signal processing [2]–[3] and wavelength conversion [4]–[7]. The QD features are improved by some techniques. For example, the Rapid Thermal Annealing (RTA) in [8] helps to obtain a high internal quantum efficiency of 66.39% and low optical loss of 9.87 cm^{-1} in QD-laser. Using the strain compensation technique, the 35-dB highest chip gain was achieved in QD-SOA with 25 stacked QD layers at 400-mA bias current [9] based on previous works [10]–[11]. In addition, QD-SOA can operate at very high bit rates up to 40 Gb/s and support several modulation formats, such as 8-PSK [5], 16-QAM [5], [12], and PAM4 [6]–[7]. Also, the nonlinear effects like Cross Gain Modulation (XGM) and Four-Wave-Mixing (FWM) were applied in wavelength conversion up to 40 Gb/s bit rate [4]–[7], while the Cross Phase Modulation (XPM) effect was used in all-optical signal processing such as logic XOR & AND gates, 2x2 switches, and D flip-flop. Besides, the input polarization dependence of QD-SOA was resolved by using the strain-controlled columnar QDs technique to be a polarization-insensitive QD-SOA as in [13].

According to the burst-mode upstream transmission in NG-PON2 [14], SOAs can be placed between Optical Network Unit/Optical Network Terminal (ONU/ONT) and Optical Distribution Network (ODN) to increase the power budgets of access links as well as a trunk line in between ODN and Optical Line Terminal (OLT). Reference [15] demonstrated the configurations of a bi-directional SOA at OLT: single SOA per downstream channel as a booster amplifier and a preamplifier SOA followed by avalanche photodiode, to give the best signal performance. In [16], QD-SOAs were applied in T-band (1000–1260 nm) WDM/TDM access network, as path switches for self-restoring system because of fast response and power loss compensation. Also, QD-SOAs were used in GPON with 1.5-μm downstream & 1.3-μm upstream transmissions to increase distance of 60 km and 32 users [17]. To gain more budget, the cascaded SOAs were proposed. In [18], a non-gated parallel cascade of linear SOAs was set up in long-reach-high-split PON to support 100 km and 2048 users. Moreover, the cascaded

Manuscript received August 26, 2021; revised November 9, 2021; accepted December 20, 2021. Date of publication December 28, 2021; date of current version January 11, 2022. *(Corresponding author: Duang-rudee Worasucheep.)*

Budsara Boriboon was with the Chulalongkorn University, Bangkok 10330, Thailand. She is now with the National Institute of Information and Communications Technology, Tokyo 184-8795, Japan (e-mail: budsara@nict.go.jp).

Duang-rudee Worasucheep is with the Chulalongkorn University, Bangkok 10330, Thailand (e-mail: duangrudee.w@chula.ac.th).

Satoshi Shimizu, Satoshi Shinada, Hideaki Furukawa, Atsushi Matsumoto, Kouichi Akahane, Naokatsu Yamamoto, and Naoya Wada are with the National Institute of Information and Communications Technology, Tokyo 184-8795, Japan (e-mail: sshimizu@nict.go.jp; sshinada@nict.go.jp; furukawa@nict.go.jp; a-matsumoto@nict.go.jp; akahane@nict.go.jp; naokatsu@nict.go.jp; wada@nict.go.jp).

Digital Object Identifier 10.1109/JPHOT.2021.3138492

TABLE I
CHARACTERISTICS OF 3 SOAS: SOA#1, SOA#2, AND QD-SOA

Optical Amplifier	Bias Current	3-dB Bandwidth	ASE Peak λ	Small Signal Gain	Saturation Output Power	Saturation Input Power	Saturation Input Power (Mod.)	Noise Figure (P_{in}= –20 dBm)
SOA#1	308 mA	72 nm	1521 nm	14.8 dB	9.2 dB	–2.6 dBm	–6.0 dBm	7.10 dB
	360 mA	72 nm	1516 nm	17.0 dB	9.8 dB	–4.2 dBm	–7.0 dBm	6.70 dB
SOA#2	285 mA	59 nm	1546 nm	14.3 dB	5.6 dB	–5.6 dBm	–9.0 dBm	9.92 dB
	332 mA	60 nm	1551 nm	17.0 dB	6.5 dB	–7.5 dBm	–12.0 dBm	9.58 dB
QD-SOA	320 mA	42 nm	1504 nm	14.5 dB	7.3 dB	–4.2 dBm	–8.5 dBm	4.87 dB
	400 mA	43 nm	1500 nm	17.0 dB	8.0 dB	–6.0 dBm	–10.8 dBm	4.59 dB

SOAs were used in PAM4 transmission of PON uplink with 1024 splits & 70 km [19]. In case of QD-SOA, the performance of 11-cascaded QD-SOAs were evaluated in recirculating loop as in [20], showing the Q-factor less than 10^{-9} BER.

Our QD-SOA is in-house developed having almost the same structure as in [9]. It has ridge structure with active InAs QDs separated by InGaAlAs spacing layers on InP(311)B substrate grown by Molecular Beam Epitaxy. To fabricate highly stacked QD layers, the strain compensation technique is applied. The cladding layers are n- and p-InAlAs. An insulator layer is Benzo Cyclo Butene. Both p- and n-contact electrodes are coated by Ti-Pt-Au.

In this paper, we compare the performances of our QD-SOA versus 2 conventional SOAs (SOA#1 & #2) in 40 Gb/s per channel of upstream transmission for future access network. Based on NG-PON2 [21], the 1530-nm wavelength is chosen for all setups. First, we measure the SOA's characteristics: 3-dB bandwidth & peak wavelength of Amplified Spontaneous Emission (ASE) spectra, small-signal gain, saturation output & input, and NF, including the response time and data pattern effect. Next, we evaluate the performance of single SOA transmission by BER measurements in 6 combination cases: splitter 1:8, 1:16 & 1:32, and with & without 20-km SMF. The BER plot versus SOA's input reveals its Input Power Dynamic Range (IPDR). Also, the two-cascaded SOA transmission is set up in 4 cases: splitter 1:32 +40-km SMF, 1:128 +20-km, 1:32 +20-km, and only 1:128 splitter. SOA#1 is fixed as the 1st-stage SOA due to its highest saturation output. Either SOA#2 or QD-SOA is placed as the 2nd-stage SOA to compare their performances. Finally, we compute the BERs according to theoretical equations, and compare to experimental results in the same BER plots versus SOA's input, in order to confirm the Optical Signal to Noise Ratio (OSNR) degradation and data pattern effect.

II. SOA'S CHARACTERISTICS

All parameters of SOA#1, SOA#2, and our QD-SOA are measured as shown in Table I. For a fair comparison, their bias currents are set at different values as listed in the 2nd column of Table I, since they will be later applied in different transmission cases for their exact same gains: a lower gain of ∼14.5 dB and a higher gain of 17 dB.

A. Experimental Setup

Fig. 1 shows our block diagram. A Laser Diode (LD), which is a tunable Distributed Feedback (DFB) laser, emits 1530-nm wavelength without data modulation. The SOAs' input power and polarization are adjusted by a Variable Optical Attenuator (VOA) and a Polarization Controller (PC), respectively. The SOAs' output spectra are recorded by an Optical Spectrum Analyzer (OSA) with 0.1-nm resolution bandwidth, and then all parameters are found. In case of the 3-dB bandwidth measurement, no input is needed.

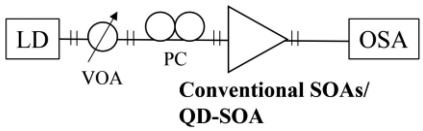

Fig. 1. Block diagram of characteristic measurement.

B. Experimental Results

Table I lists all parameters of 3 SOAs. Their details will be discussed in the following sub-sections. In addition, the saturation input powers without and with 40 Gb/s data modulation are included in the 7th and 8th columns, respectively. By a definition, the saturation input/output is power level that causes its gain to reduce by 3 dB from the highest small-signal gain. Any input/output above it will be in saturation operation. In this case, the higher saturation inputs without data modulation are used to compare SOA's characteristic, while the lower saturation inputs with data modulation are applied in Section III SOA's Response Time & Data Pattern Effect.

1) ASE Peak Wavelength and 3-dB Bandwidth: All 3 SOA's output spectra have operating ranges covering 1530 nm. The 3-dB bandwidth and ASE peak wavelength are listed in the 3rd & 4th columns, respectively. Clearly, SOA#1 has the widest bandwidth of 72 nm. Fig. 2 shows our QD-SOA's ASE spectra at 320 and 400-mA currents. Its 3-dB bandwidths are the narrowest (43 nm), but still wider than 35 nm of typical EDFAs. In this case, the QD structure is almost homogeneous QDs, resulting in its high gains but with a narrow bandwidth. The design of our QD-SOA aims to amplify wavelengths outside the C-band (1530–1565 nm) of EDFAs.

2) Gain, Saturation Output & Input Powers: More gain and higher saturation output are the keys to boost a link's budget. Table I column 5–8 list the small-signal gain, saturation output, and saturation input powers (without & with Mod.). Among all saturation outputs, SOA#1 has the highest power of 9.8 dBm at 360-mA current. Fig. 3 plots the gain curves of QD-SOA at 320 and 400-mA currents, showing both small-signal gain and saturation output (*Pout, sat*). Its 8-dBm saturation is in between

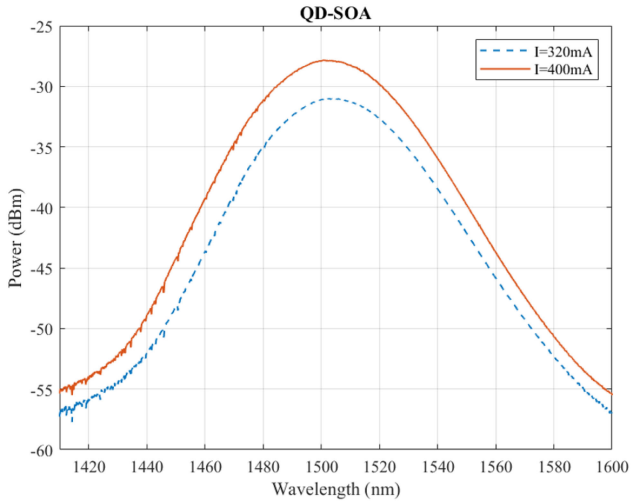

Fig. 2. ASE spectra of QD-SOA at 320 & 400-mA.

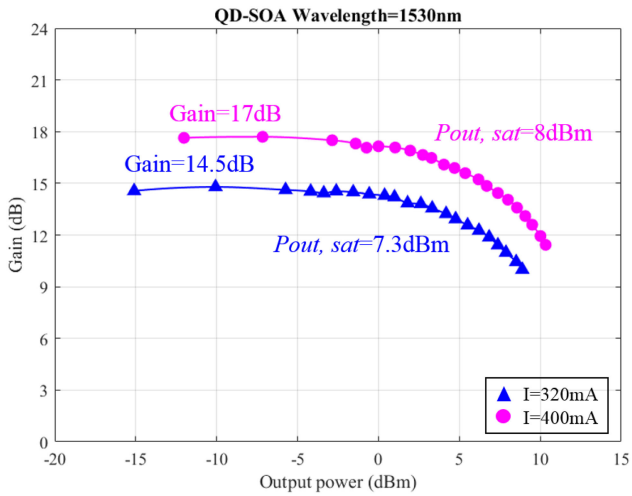

Fig. 3. Gain and saturation output power of QD-SOA.

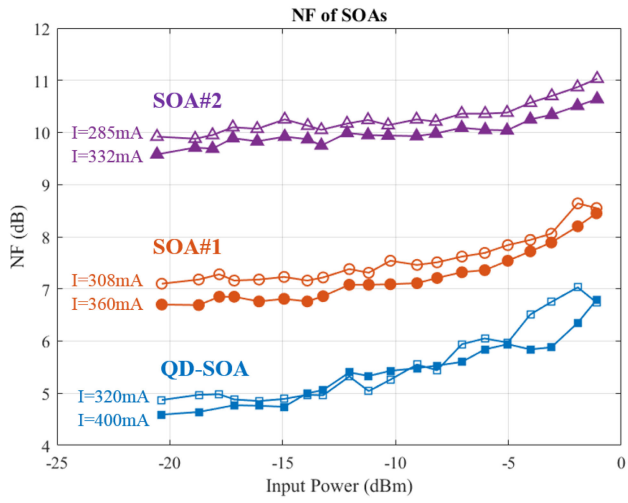

Fig. 4. NFs of 3 SOAs at lower and higher bias currents.

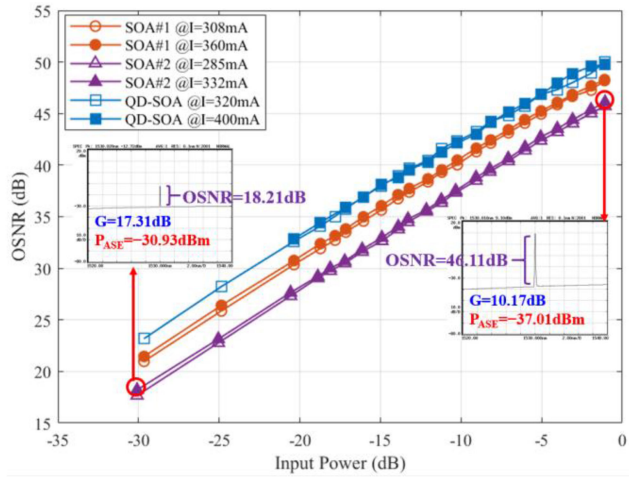

Fig. 5. Output OSNRs versus input power of 3 SOAs.

those outputs of 2 conventional SOAs. However, this saturation output of QD-SOA can be increased up to 24 dBm [22] by the tapered gain section [23].

3) Noise Figure (NF): Last column of Table I lists all NFs measured by OSA at –20 dBm input of SOA. The NFs of SOA#1 & #2 are about 8 & 10 dB, as reported in their data sheets [24]–[25]. When SOA's input increases above saturation input, its NF gradually rises as seen in Fig. 4. Evidently, our QD-SOA gives the lowest NF across all inputs due to its higher OSNR at output as plotted in Fig. 5. For example, in case of SOA#2 at 332-mA current, two insets in Fig. 5 shows the lowest $OSNR_{out}$ of 18.21 dB at –30.09-dBm input and the highest $OSNR_{out}$ of 46.11 dB at –1.07-dBm input.

According to the original equation of NF in [26], it shows no wavelength dependence since it is a ratio between the electrical SNR at input and the SNR at amplifier output. But in this case, all NFs are measured optically by OSA for comparison among 3 SOAs. Based on [27] that considering only the signal-ASE beat noise and 100% quantum efficiency, the NF equation is revised to be in terms of the spectral density of ASE noise, S_{ASE}, over $Gh\nu$, where G is SOA's gain, h is Planck's constant ($= 6.626 \times 10^{-34}$ J·s) and ν is frequency of input wavelength. Here, it gets converted to be (1), by replacing S_{ASE} with a ratio of ASE noise, P_{ASE}, over frequency band, B_{ref}, which is a conversion of OSA's resolution bandwidth ($B_{ref} = (c\Delta\lambda)/\lambda^2$). And, replacing G with SOA's output, P_{out}, divided by input, P_{in}. Last, replacing a ratio of P_{out} to P_{ASE} by $OSNR_{out}$. As a result, the NF in (1) depends on P_{in}, $OSNR_{out}$ and wavelength λ (through $\nu = c/\lambda$).

$$NF = \frac{2P_{in}}{h\nu B_{ref}} \left[\frac{1}{OSNR_{out}}\right] \quad (1)$$

The NF results in Fig. 4 are in agreement with (1). They are almost constant across small-signal gain region due to the linearity of output OSNR over low inputs as shown in Fig. 5. But they slowly increase across saturation region, because the OSNR slightly tapers off over high inputs. The lower current gives lower OSNRs as in Fig. 5 and higher NFs as in Fig. 4.

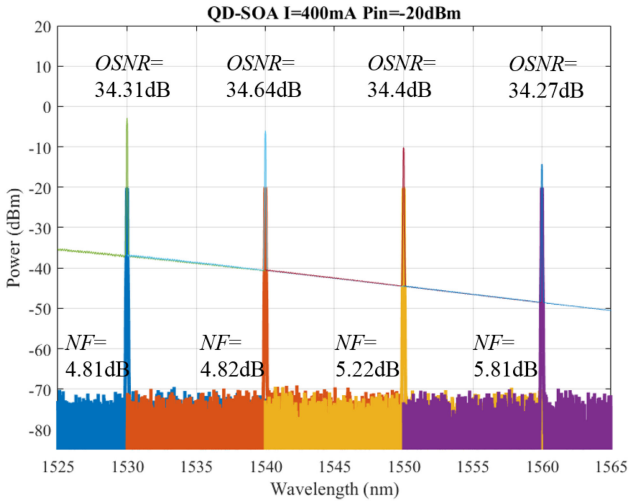

Fig. 6. Input and Output spectra of QD-SOA.

The NF equation in OSA user manual [28] is given in (2). It can be derived by replacing 3 parameters in NF equation [27]: ($S_{ASE} = P_{ASE}/B_{ref}$), ($B_{ref} = (c\Delta\lambda)/\lambda^2$) and ($\nu = c/\lambda$). Unlike (1), the NF in (2) do not have a factor of 2, because the ASE noise is usually assumed to be unpolarized [27].

$$NF = \frac{1}{hc^2} \times \frac{\lambda^3}{\Delta\lambda} \times \frac{P_{ASE}}{G} \tag{2}$$

The wavelength dependency of NF in (2) is demonstrated by measuring input and output spectra of 3 SOAs at 1530, 1540, 1550 and 1560-nm wavelengths from a tunable LD. Fig. 6 shows the spectra of QD-SOA at 400-mA current and –20 dBm input. All NF results of QD-SOA and conventional SOAs show their minor wavelength dependency.

III. SOA's Response Time & Data Pattern Effect

The SOAs are well-known to have faster response times than those fiber-based amplifiers, like EDFA. Thus, they are suitable for burst-mode applications, for example as amplifiers in upstream PON transmission. However, when operating as boosters with high input powers (aka. in saturation region), the unwanted overshoots due to data pattern effect may occur. And this will affect the length of overhead bits in timeslot sharing of upstream PON. In this study, we compare the response times of SOA#1, SOA#2, and QD-SOA at lower & higher bias currents in both small-signal gain and saturation regions.

A. Experimental Setup

In Fig. 7, data pattern is generated by 4 Ch x 10 Gb/s Pulse Pattern Generator (PPG), 4 to 1 Multiplexer (MUX), 1530-nm LD, and Mach-Zehnder Modulator (MZM), to be the long consecutive 64 zeros and 64 ones alternatively. Later, this same setup was used for the BER tests of 40 Gb/s Pseudo-Random Binary Sequence (PRBS) data in Section IV Bit Error Rate (BER). The input polarizations of MZM and SOA are adjusted by PCs, while the input powers of SOA and Digital Communications Analyzer (DCA) are varied by VOAs. The SOA's output waveforms are detected by a photodetector (PD) and an electrical port of DCA

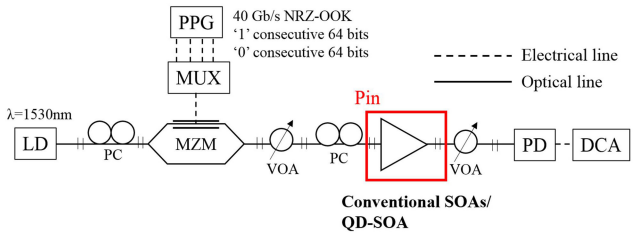

Fig. 7. Block diagram to measure the response times.

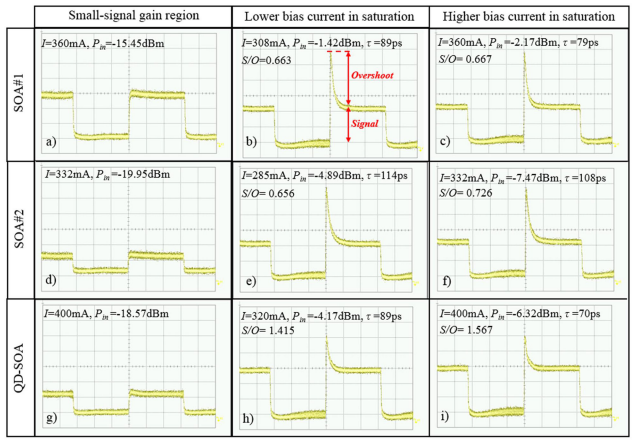

Fig. 8. Output waveforms of 3 SOAs: small-signal gain, and saturation at lower and higher bias currents.

with 40 GHz and 50 GHz bandwidth, respectively. Based on the saturation input (Mod.) in Table I column 8, each SOA's input is set accordingly at a lower power for the small-signal gain operation, and at a higher power (4–5 dB above) for the saturation operation.

B. Experimental Results

Fig. 8 compares the output responses of 3 SOAs. The 1st column of small-signal gain operation at higher current (omitting same results at lower current) has no overshoot, and thus no data pattern effect. But they are prominent under saturation operation as in the 2nd & 3rd columns. So, we focus on them to determine the response time. Fig. 8(b) illustrates the amount of Signal versus Overshoot that we define as *Signal to Overshoot ratio* (*S/O*). The higher *S/O* in QD-SOA reflects less pattern effect, while both SOA#1 & SOA#2 show strong effect.

The response time, τ, can be approximated by a decay exponential equation as in Fig. 9 and (3), where y is voltage, V_{SS} is steady-state voltage, A is peak amplitude, and t is time in picosecond.

$$y = V_{SS} + Ae^{\frac{-t}{\tau}}. \tag{3}$$

All response times and *S/O* under saturation are listed in Fig. 8. QD-SOA gives the fastest response of 70 ps and the highest *S/O* = 1.567 at higher bias current. For a better view, Fig. 10 plots the decay exponential curves estimating those 3 waveforms in the last column of Fig. 8. Clearly, the QD-SOA has a lower

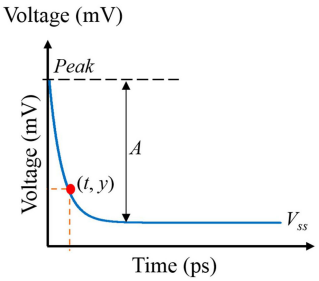

Fig. 9. Parameters of a decay exponential curve.

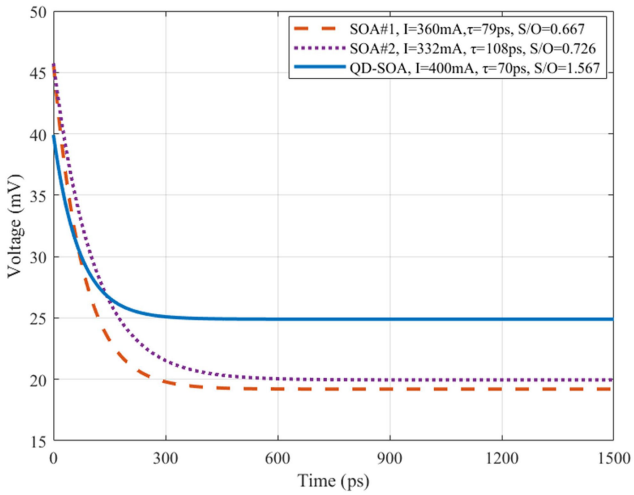

Fig. 10. Estimated decay exponential curves of 3 SOAs at higher bias currents.

overshoot and faster recovery than conventional SOAs due to the Ground State that gives ultra-fast recovery time within a few picoseconds, while a typical recovery time of SOA is longer than 10 ps [29]. In this case, our results display the overall response time without separating the ultra-fast or fast parts from slow response, unlike a clear picture shown in [30].

The overshoot responses of 3 SOAs under saturation at different input powers and bias currents are also studied. For example, Fig. 11 compares the outputs of SOA#1. In Fig. 11(a) and (b) at same input, the higher current gives more overshoot and a lower response time owing to more carrier density injected to an active layer, and thus higher population inversion and faster refilling carrier density [31]. In Fig. 11(c) and (d) at same current, the higher input causes more overshoot and reduces response time because of its higher stimulated emission rate [32].

A higher overshoot is related to the severe frequency chirp [33], which depends on the linewidth enhancement factor, α, as given in (4) [34],

$$\alpha = -\frac{4\pi}{\lambda}\frac{(\partial n/\partial N)}{\Gamma A_g} \tag{4}$$

where n is refractive index, N is carrier density, λ is wavelength, Γ is confinement factor, and A_g is differential gain ($A_g = \partial g/\partial N$, g is material gain). When operating in saturation region, this α is positive due to carrier depletion ($\Delta N < 0$) [34] that causes

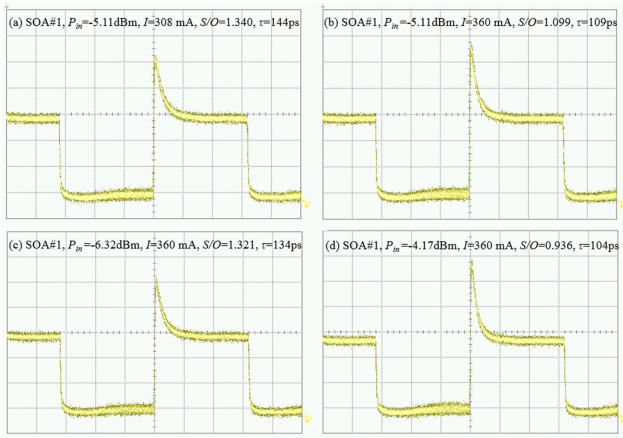

Fig. 11. Outputs of SOA#1: (a) lower and (b) higher current at –5.11 dBm input, and (c) lower and (d) higher input at 360-mA (higher) current.

a change in refractive index. The overshoot or pattern effect gets worse under high input power and bias current as shown in Fig. 11. In [35], the QD-SOA has a lower α than conventional SOA, and hence less frequency chirp.

IV. Bit Error Rate

The performances of 2 conventional SOAs and QD-SOA in a network link are identified by BER in 2 cases: single SOA and two-cascaded SOA. Back-to-Back (B-B) cases are also included as reference. Link#1 and Link#2 both consist of 20-km Standard Single Mode Fiber (SSMF) and Dispersion Compensation Fiber (DCF) to remove Chromatic Dispersion (CD). Their total losses are 6.69 and 8.43 dB, respectively. The BER performance depends on SOA's input power, and thus the IPDR of 3 SOAs are measured. Lastly, the theoretical equations are presented to compute BERs and verify experimental results.

A. Experimental Setup

Fig. 12 shows 4 block diagrams using the same transmitter as in Section III. All 40-Gb/s data are PRBS23, except in Fig. 12(d) using PRBS15 for better BERs [36]. The input of receiver (Rx) is varied by VOA#1 and split by 10-dB coupler to be clock & data signals in upper & lower paths, respectively. The upper path with less power needs an EDFA. Next, both clock & data signals are detected by 2 PDs and amplified by Driver Amplifiers before entering 1 to 4 De-multiplexer (DEMUX). The 40 GHz clock is retrieved by a Clock Recovery (CR) for BER measurement at Error Detector (ED). Fig. 12(a) studies only the CD effect in Link#1 & #2. Fig. 12(b) focuses on the BER and IPDR of either SOA#1, SOA#2 or QD-SOA without a link. The ASE noise of SOA is limited by a 2-nm Tunable Optical Band Pass Filter (TOBPF). Fig. 12(c) combines SOA with Link#1, so called the single SOA transmission, and uses VOA#2 as 1:N splitter (N = 8, 16, and 32). Fig. 12(d) adds Link#2 in the two-cascaded SOA transmission: SOA#1 followed by SOA#2 or QD-SOA. Here, VOA#3 acts as 1:8 splitter between 1st & 2nd stage SOAs, while

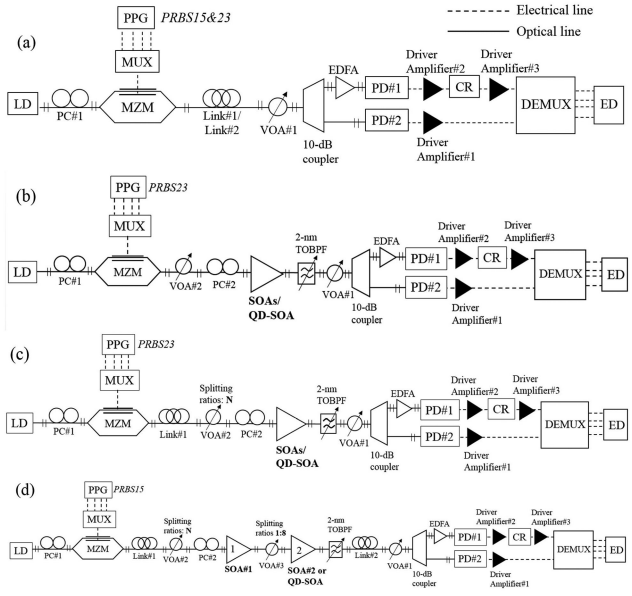

Fig. 12. Block diagrams: (a) link w/o SOA, (b) single SOA w/o link, (c) link w/ single SOA, and (d) Link#1&2 w/ two-cascaded SOA.

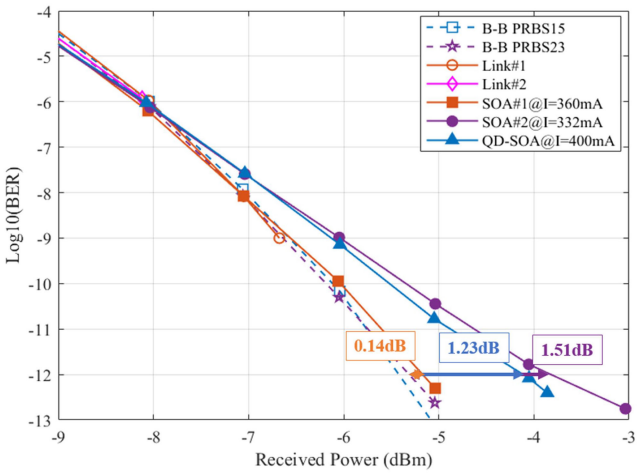

Fig. 13. BER curves of different cases: B-B (PRBS15 & 23), Link#1, Link#2, SOA#1, SOA#2, and QD-SOA.

VOA#2 reduces its splitting ratio down to 4 and 16 due to limited link budget.

B. Chromatic Dispersion (CD) Compensation in Link#1 & #2, and BER Performances of 3 SOAs

Based on Fig. 12(a) and (b), the BER results of Link#1, Link#2, and single SOA (SOA#1, SOA#2 or QD-SOA) are plotted in Fig. 13, with B-B cases of PRBS15 & 23. Since Link#1 & #2 have different losses, their budget limits the BER results below received powers of –6.67 & –8.12 dBm, respectively. The partial curve of Link#1 case follows B-B curves, proving the DCFs can compensate CD of SSMFs. All SOAs are set at higher bias currents and same input of –16.94 dBm. In Fig. 13, the power penalties of SOA#1, SOA#2, and QD-SOA at 10^{-12} BER are 0.14, 1.51, and 1.23 dB respectively. SOA#1 has the least penalty owing to its highest saturation output of 9.8 dBm as in Table I, and thus having low data pattern effect.

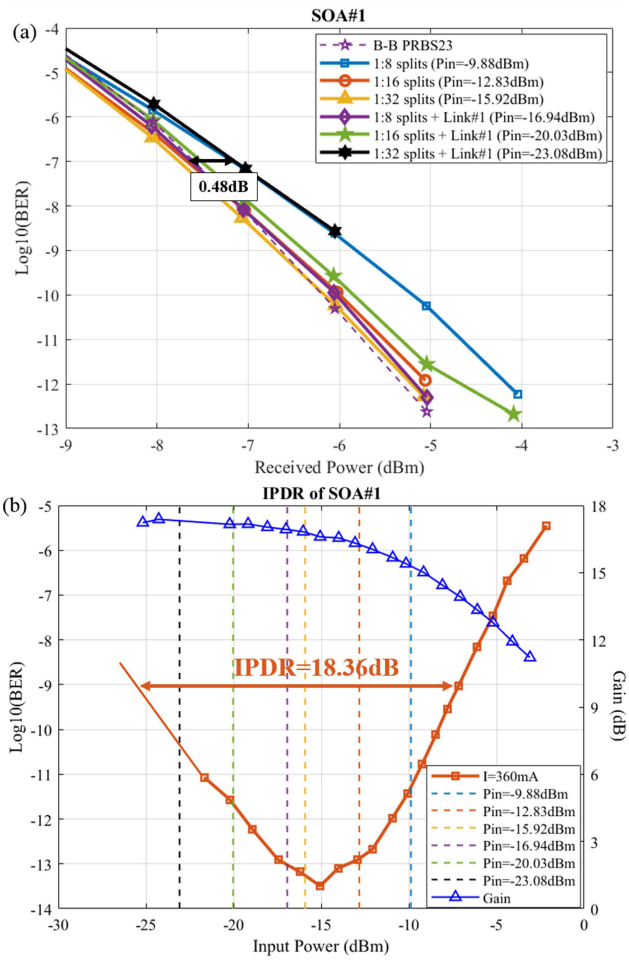

Fig. 14. SOA#1 at 360 mA: (a) BER curves of 6 cases and (b) BER plot versus SOA's input showing IPDR (square) & Gain plot (triangle).

C. Single SOA Transmission & Input Power Dynamic Range (IPDR)

As in Fig. 12(c), we evaluate the 40 Gb/s upstream transmission of each SOA with access Link#1. Also, the BER results versus SOA's input is plotted to identify its IPDR. All SOAs are set at higher bias currents, with & without Link#1, and 3 splitting ratios: 1:8, 1:16 & 1:32. These ratios have different Insertion Losses (IL), which will vary SOA's input. Hence, there are 6 cases: i) 8 splits, ii) 16 splits, iii) 32 splits, iv) 8 splits with Link#1, v) 16 splits with Link#1, and vi) 32 splits with Link#1.

1) SOA#1 Transmission & IPDR: Fig. 14(a) shows the BER curves of B-B (PRBS23) and 6 cases of different SOA's inputs due to IL of splitter and total loss of Link#1. Case i - v) have penalties of 1.16, 0.32, 0.1, 0.15, and 0.68 dB at 10^{-12} BER, respectively. But, in case vi), no BER below 10^{-9} could be measured due to a high IL of 32 splits. So, it shows 0.48-dB penalty at 10^{-7} BER instead. Based on these BER curves, they

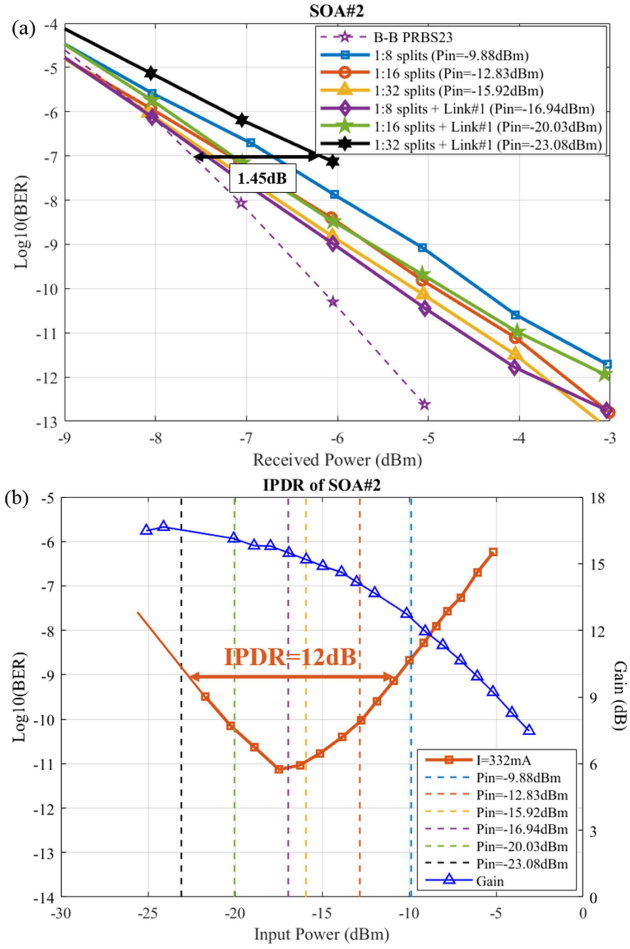

Fig. 15. SOA#2 at 332 mA: (a) BER curves of 6 cases and (b) BER plot versus SOA's input showing IPDR (square) & Gain plot (triangle).

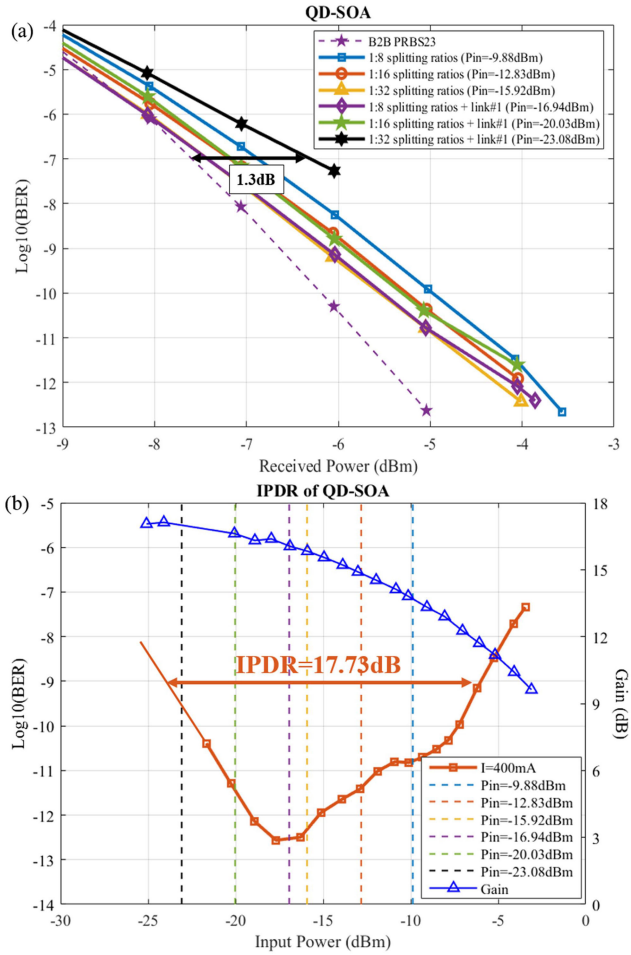

Fig. 16. QD-SOA at 400 mA: (a) BER curves of 6 cases and (b) BER plot versus SOA's input showing IPDR (square) & Gain plot (triangle).

rely on the SOA's inputs. Next, using the setup in Fig. 12(b) to find IPDR, we measure BERs at many SOA's inputs while the received power at receiver (Rx) is kept at –4 dBm by VOA#1. Fig. 14(b) shows the lowest BER of 3.9×10^{-14} at SOA's input of –15.11 dBm, and the IPDR of 18.36 dB at 10^{-9} BER. The left side of BER curve gets worse due to OSNR degradation, similar to Fig. 5 [37]; whereas the right side gets worse due to data pattern effect. Notice that the BER results in Fig. 14(a) with 6 different SOA's inputs are related to the BER curve in Fig. 14(b), shown as vertical dash lines. So, case i & ii) are dominated by pattern effect, while case iii - vi) are dominated by OSNR degradation. Furthermore, the gain curve is included in Fig. 14(b), showing its 3-dB saturation input power at –7 dBm, same as listed in the 8th columns of Table I. The optimal point with minimum BER has its gain and output power at 16.6 dB and 1.49 dBm, respectively.

2) SOA#2 Transmission & IPDR: SOA#2 is assessed under same conditions as SOA#1. All BER curves are displayed in Fig. 15(a), being worse than those of SOA#1 due to the higher NF and lower saturation output. Case i - v) have higher penalties of 2.55, 1.84, 1.61, 1.52, and 2.32 dB at 10^{-12} BER, respectively. Again, in case vi), no BER below 10^{-8} could be measured. So, it shows 1.45-dB penalty at 10^{-7} BER. In Fig. 15(b), SOA's input of –17.47 dBm gives the lowest BER of 7.7×10^{-12}. Its IPDR at 10^{-9} BER is 12 dB, much less than 18.36 dB of SOA#1. Also, it implies worse pattern effect (case i-iii) and OSNR degradation (case v-vi). Again, Fig. 14(b) also shows the gain curve. The gain and output power at the optimal point are 15.6 dB and –1.87 dBm, respectively.

3) QD-SOA Transmission & IPDR: Like SOA#1 & #2, the same conditions and 6 cases are set for QD-SOA. Its BER curves are given in Fig. 16(a). They are slightly better than those of SOA#2, and much lower BERs across high received powers ($>$ –5 dBm). Still, SOA#1 has the best BERs owing to its high performance. In fact, there are several techniques to improve SOAs to be high performance [38]. The penalties of case i - v) are 1.5, 1.39, 1.03, 1.24, and 1.61 dB at 10^{-12} BER, respectively. Again, in case vi) without BER below 10^{-8} shows 1.3-dB penalty at 10^{-7} BER. All penalties are less than those of SOA#2, but not as good as SOA#1. Same as SOA#2, case i - iii) are dominated by pattern effect, and case v - vi) are dominated by OSNR degradation. In Fig. 16(b), QD-SOA's input of –17.69 dBm gives the lowest BER of 3.0×10^{-13}. Its IPDR at 10^{-9} BER is 17.73 dB, close to 18.36 dB of SOA#1. When the input

is higher than –8 dBm, its BERs are better than those of SOA#1. In other words, our QD-SOA can operate over high input powers with less pattern effect as compared to conventional SOAs. Also, the gain curve is plotted in Fig. 14(b). The gain and output power are 16.2 dB and –1.49 dBm, respectively, at the optimal point.

D. Two-Cascaded SOA Transmission

Any access network will require the higher budget to support more users (splitter) and longer distance. Thus, the two-cascaded SOA is proposed to raise such budget. Its block diagram for an upstream transmission is already presented in Fig. 12(d). Link#1 acts as an access link connecting ONU/ONT to ODN, whereas Link#2 acts as a main link connecting ODN to OLT. In this case, our ODN consists of a 1:N splitter (N = 4 or 16) after Link#1, and a fixed 1:8 splitter in between 1st & 2nd-stage SOA. SOA#1 is chosen over SOA#2 as the 1st-stage SOA on account of its overall high performance: high gain, high saturation output, superior BER results, larger IPDR, and moderate NF. Plus, to reduce cost, no TOBPF is inserted between 1st and 2nd-stage SOAs, hence this 1st-stage SOA must have the best characteristics. The current of SOA#1 is set at typical 500 mA (higher than in Table I) for more gain of 19 dB. The 2nd-stage SOA is either SOA#2 or QD-SOA, both set at higher currents. Since the 2-cascaded SOA transmission has worse ASE noise, PRBS15 is used instead of PRBS23 in these 4 new cases: a) 32 splits with Link#1 & #2, b) 128 splits with Link#2, c) 32 splits with Link#1, and d) only 128 splits. Case a) is common (N = 4), while case b) removes access Link#1 to gain users (N = 16). In contrast, case c) & d) remove main Link#2 as if OLT is placed nearby ODN, and the 2nd-stage SOA acts as a preamplifier. Based on the minimum BER in a BER plot versus SOA#1's input at 500-mA current (excluding here, but similar to Fig. 14(b)), the input of 1st-stage SOA#1 is fixed at –14.02 dBm. With 19 dB gain, its output is about 5 dBm. After 1:8 splitter (IL ≈ 9 dB), the input of 2nd-stage SOA#2 or QD-SOA is about –4.84 dBm. Later, in Section 3) Verify Performance of 2nd-stage SOA, the fixed 1:8 splitter is replaced by 1:16 & 1:32 to vary input of 2nd-stage SOA, resulting in 6 combination cases: SOA#2 with 8, 16 & 32 splits, and QD-SOA with 8, 16 & 32 splits. All BER curves are measured to report the corresponding power penalties of different splitting ratios (8, 16 & 32), as well as the output powers of 2nd-stage SOA.

1) Two-cascaded SOA#1 & SOA#2: Fig. 17 plots the BER curves of B-B (PRBS15) and 4 cases. Due to limited budget, the highest received power is –3 dBm. So, the penalty is read at 10^{-6} BER instead for case a) – d) to be 3.88, 3.53, 2.76, and 2.69 dB, respectively. Case a) has the most penalty due to its longer 40-km SSMF despite CD compensation by DCF. In case b) & d), when Link#1 is removed for more splits (1:128), its total loss of 6.69 dB is almost equal to an extra IL (∼6 dB) from replacing 1:4 splitter by 1:16. So, the input of 1st-stage SOA#1 is unchanged, resulting in similar BER curves. But, when Link#2 is removed as in case c) & d), their penalties reduce about 1 dB, possibly as a result of less perfect CD compensation than Link#1. Now, focusing at –4 dBm received power, all BER results are between 10^{-7} and 10^{-6} BER in agreement with the BER in Fig. 15(b)

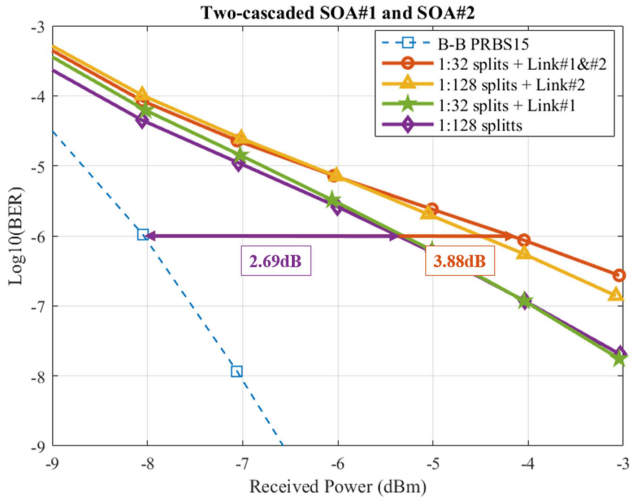

Fig. 17. BER curves of 2-cascaded SOA#1 & SOA#2.

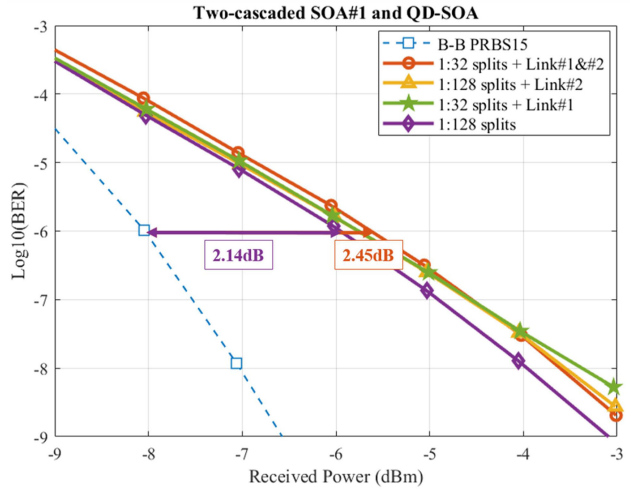

Fig. 18. BER curves of 2-cascaded SOA#1 & QD-SOA.

read at SOA#2's input of –5 dBm (close to –4.84 dBm input power of 2nd-stage SOA).

2) Two-Cascaded SOA#1 & QD-SOA: Likewise, Fig. 18 shows the BER curves with penalties at 10^{-6} BER in case a) – d) to be 2.45, 2.31, 2.31 & 2.14 dB respectively. Again, case a) has the most penalty, and case d) with only splitters has the least penalty. In case c) & d), the imperfect CD compensation of Link#2 shows little penalties. Remarking at –4 dBm received power, all BERs are between 10^{-8} and 10^{-7} BER, which are close to the BER in Fig. 16(b) at –4.84 dBm input of QD-SOA.

The performance of 2-cascaded SOA#1 & QD-SOA is better than 2-cascaded SOA#1 & SOA#2, because QD-SOA has lower BERs than SOA#2 according to Figs. 15(b) and 16(b) when operating at high input as 2nd-stage SOA. Plus, it has higher saturation output and less pattern effect when operating in saturation as shown in Section III. Based on our experiments, we achieve either 40-km SSMF with 32 splits or 128 splits without a long SSMF. Thus, this scenario of 2-cascaded SOAs

TABLE II
ALL PARAMETERS AND VALUES FOR 2ND-STAGE SOA

2nd-stage SOA	Splits	P_{out} (dBm)	*Penalty* @10^{-7} BER (dB)	P_{out}–*Penalty* @ 10^{-7} BER (dB)
SOA#2	8	5.61	1	4.61
	16	3.93	–0.4	4.33
	32	2.78	–1	3.78
QD-SOA	8 [a]	6.23	0	6.23
	16	4.32	–0.9	5.22
	32	2.75	–1	3.75

[a]Reference

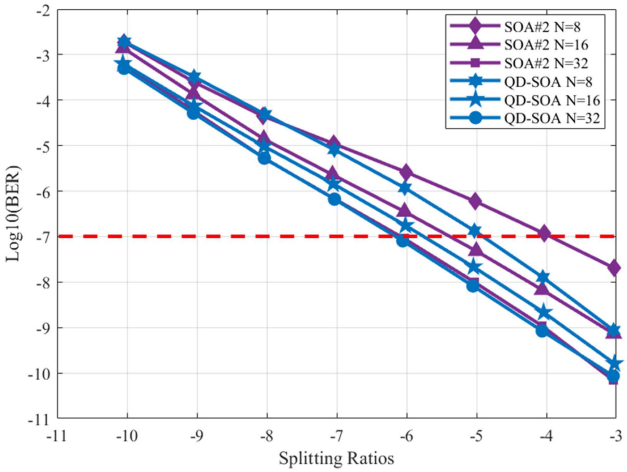

Fig. 19 BER curves of 2nd-stage SOA with N splits.

can be implemented to increase the power budget of upstream transmission.

3) Verify Performance of 2nd-Stage SOA: We verify the performance of 2nd-stage SOA (SOA#2 or QD-SOA) by varying a splitting ratio between 1st & 2nd-stage SOAs: 8, 16, and 32; while the input and output of 1st-stage SOA#1 are fixed at –14.02 & 5 dBm, respectively. So, the inputs of 2nd-stage SOA are –4.84, –7.91 & –10.87 dBm for 8, 16, and 32 splits, respectively. Two parameters of 2nd-stage SOA are focused. First, the higher output (P_{out}) with same input reflects more power budget. Second, the lower penalty represents better performance, depending on SOA's input. Consequently, we define (P_{out} – *Penalty*) @ 10^{-7} BER to compare the performance of 2nd-stage SOA; of course, the higher the better. Table II lists all parameters. Based on the saturation outputs in Table I, our QD-SOA gives a higher output P_{out} than SOA#2 when operating at high input, corresponding to a lower split of 1:8. Fig. 19 shows the BER curves of 6 cases. All Penalty @ 10^{-7} BER in Table II are measured relative to the reference case: QD-SOA+8split. For example, the case of SOA#2+8split has 1 dB more penalty than the reference. But the case of SOA#2+16split has 0.4 dB less penalty than the reference (a negative value in Table II).

In the last column of Table II, QD-SOA with 8 and 16 splits have very high (P_{out} – *Penalty*) as compared to SOA#2, because of its higher outputs and less penalties when operating at high inputs. Especially, in the scenario of 2-cascaded SOAs without a splitter in between SOAs, the high output of 1st-stage SOA will demand 2nd-stage SOA to support such high input with less signal degradation. Hence, the QD-SOA will give the best performance at high input (in saturation region).

TABLE III
PARAMETERS AND VALUES FOR BER COMPUTATION

Parameter	Symbol	Value	Unit
Electron Charge	q	1.6021×10^{-19}	C
Responsivity	R	0.65	A/W
Electrical Bandwidth	B_e	40	GHz
Optical Bandwidth	B_O	2 [39]	nm
Boltzmann Constant	k_B	1.38054×10^{-23}	J/K
Temperature	T	298	K
Load Resistance	R_L	50	Ω
Dark Current	I_d	200	nA
Electrical Amplifier's NF	F_n	6.31	

E. Theoretical Equations

This section lists the equations to approximate BERs, starting with 5 noises. All parameters related to our experiments are applied to compute the Signal-to-Noise Ratio (SNR), Q-factor, and finally BERs of 3 SOAs.

1) Noise Terms: The data output of PD#2 in Fig. 12 has 5 noises [26]: shot, signal-ASE beat, ASE-ASE beat, thermal, and dark current, as in (5)–(9). All parameters and their values are declared in Table III. The first 3 noises vary with SOAs' gain G and ASE noise power P_{ASE}, in which they depend on SOAs' input power P_{in}. For instance, different values of G and P_{ASE} at the lowest and highest inputs are shown in two insets in Fig. 5. Besides, for IPDR measurements of 3 SOAs as in Fig. 12(b), the power loss from VOA#1 is represented by Attenuation Factor (AF), to maintain a received power of –4 dBm at receiver (Rx).

$$\left\langle i_{shot}^2 \right\rangle = \sigma_{shot}^2 = 2qRB_e\left[(GP_{in} + P_{ASE}) \times 10^{\frac{-AF}{10}}\right] \quad (5)$$

$$\left\langle i_{S-ASE}^2 \right\rangle = \sigma_{S-ASE}^2 = \frac{4R^2GP_{in}P_{ASE}B_e}{B_O} \times 10^{\frac{-AF}{5}} \quad (6)$$

$$\left\langle i_{ASE-ASE}^2 \right\rangle = \sigma_{ASE-ASE}^2 = \frac{4R^2P_{ASE}^2B_e}{B_O} \times 10^{\frac{-AF}{5}} \quad (7)$$

$$\left\langle i_T^2 \right\rangle = \sigma_T^2 = \left(\frac{4k_BT}{R_L}\right)B_e \quad (8)$$

$$\left\langle i_d^2 \right\rangle = \sigma_d^2 = 2qI_dB_e \quad (9)$$

2) BER Calculation: BER is related to the SNR in (10), which is a ratio of signal power of photo-current from PD#2, $<i^2{}_P>$ in (10), over a summation of 5 noises that are scaled up by a NF of electrical amplifier, F_n [40].

$$SNR = \frac{\left\langle i_P^2 \right\rangle \times E_{Pattern}}{\left(\sigma_{shot}^2 + \sigma_{S-ASE}^2 + \sigma_{ASE-ASE}^2 + \sigma_T^2 + \sigma_d^2\right) \times F_n} \quad (10)$$

$$\left\langle i_P^2 \right\rangle = \left(R \times GP_{in} \times 10^{\frac{-AF}{10}} \right)^2 \tag{11}$$

In addition, to include the data pattern effect across high inputs in a BER plot versus SOA's input, like in Fig. 14(b), we introduce $E_{Pattern}$ factor defined in (12).

$$E_{Pattern} = 10^{\left[\frac{G_{Pin} - G_{\min\_BER}}{10}\right]} \tag{12}$$

where $G_{\min\_BER}$ is gain at minimum BER, and G_{Pin} is gain at each input on the right side of minimum BER. For those inputs on the left side of minimum BER, their $E_{Pattern}$ are equal to 1. But on the right side, their $E_{Pattern}$ gradually reduce, causing less signal powers and more BERs.

Finally, the BER is computed from SNR according to (13), where *erfc* is complementary error function.

$$BER = \frac{1}{2} erfc \left[\frac{\sqrt{SNR}}{2\sqrt{2}} \right] \tag{13}$$

In the B-B case, its BER is calculated without ASE noise terms. In the next section, all computed BER points are plotted along with experimental results in the same BER plot versus SOA's input.

F. Computed BERs of SOA#1, SOA#2 & QD-SOA

From all equations in Section E and parameters in Table III, the BERs are computed at fixed –4 dBm received power with proper AFs for 3 SOAs biased at high currents. This power is same as in Section C experiments showing IPDR. Next, the gain G and ASE noise power P_{ASE}, both read from an OSA at each SOA's input P_{in}, are substituted into those equations to find 5 noises and BERs.

The computed and experimental BERs are plotted together in Fig. 20(a)–(c) for SOA#1, SOA#2, and QD-SOA. These BER curves show the OSNR degradation and pattern effect that worsen BERs on the left and right sides of minimum BER, respectively. Towards the left side, those computed BERs increase due to the higher P_{ASE} and lower OSNR, as proven by those insets in Fig. 20(a)–(c) with larger signal-ASE beat noise across lower inputs. Towards the right side, those computed BERs also rise due to the elevated shot noise across higher inputs, as illustrated by those same insets in Fig. 20(a)–(c), as well as the slow reduction of $E_{Pattern}$ factors. In case of SOA#1, these $E_{Pattern}$ decreases from 0.948 at minimum BER to 0.222 at its highest input. In case of SOA#2 and QD-SOA, their $E_{Pattern}$ decline from 0.935 to 0.129, and 0.951 to 0.182, respectively. However, comparing among 5 noises, the thermal noise is dominant as shown by those 3 insets in Fig. 20, whereas the dark current noise can be neglected. Moreover, when the inputs of 3 SOAs are above –5 dBm (approximately), the slopes of computed BERs slightly decrease due to their lower gain. In case of QD-SOA in Fig. 20(c), the experimental BERs measured between –14 and –6 dBm inputs show an almost flat slope because of its characteristics. In summary, our computed BER curves that include both OSNR degradation and pattern effect follow the tendency of experimental BER curves.

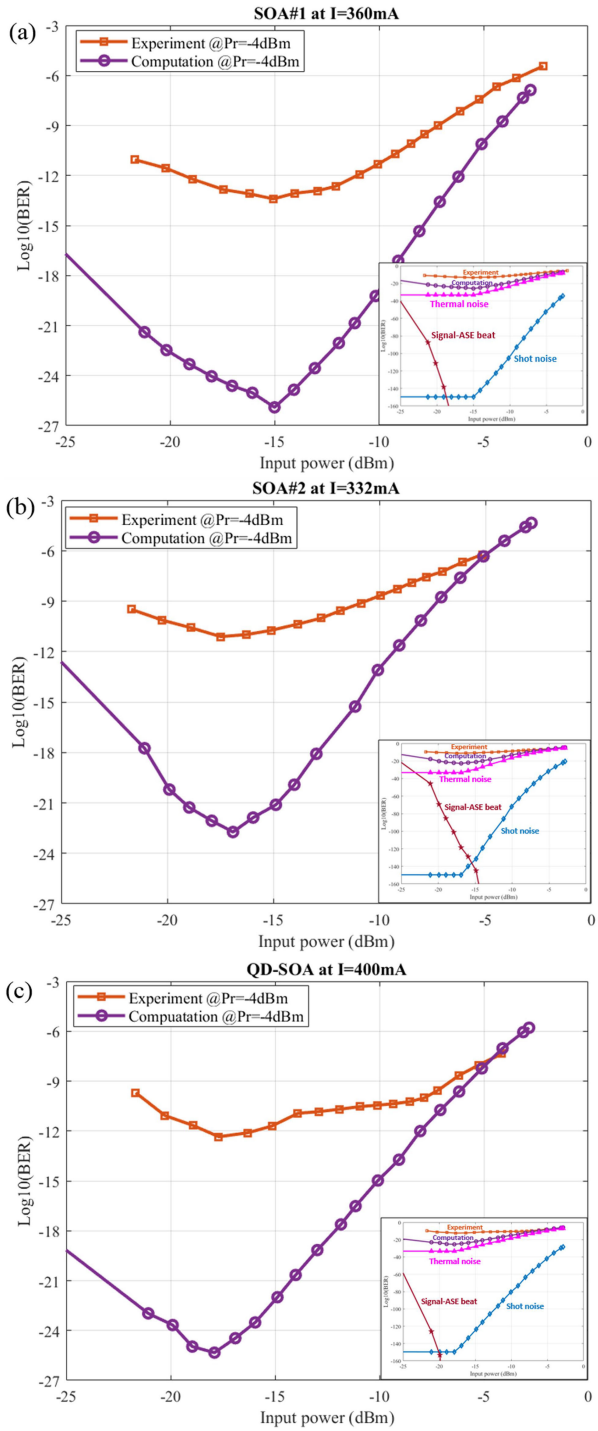

Fig. 20 Computed and experimental BERs: (a) SOA#1, (b) SOA#2, and (c) QD-SOA.

V. Conclusion

We evaluate the performances of two conventional SOAs (#1 & #2) and our QD-SOA in 1530-nm upstream transmission of 40 Gb/s access network over two 20-km SSMF with DCF (Link#1 & #2) and splitters (8, 16 & 32). From the characteristic results of 3 SOAs, our QD-SOA gives the lowest NF of 4.59 dB at –20-dB input, as well as the fastest response of 70 ps and highest *S/O* of 1.567. Hence, it is more suitable for burst-mode amplification.

Based on the single SOA transmission in 6 combination cases (3 splitters with & without Link#1), the BER curves of 3 SOAs depend on their inputs, proven by those BER plots versus SOA's input that show IPDRs. SOA#1 has the superior BER results and higher saturation output, and thus is applied as 1st-stage SOA. In the 2-cascaded SOA transmission using either SOA#2 or QD-SOA as 2nd-stage, there are 4 cases: 32 splits with Link#1 & #2, 128 splits with Link#2, 32 splits with Link#1, and 128 splits only. All BER results of QD-SOA are better than those of SOA#2, and with lower power penalties due to the higher saturation output and less pattern effect of QD-SOA. Also, we verify the performance of 2nd-stage SOA with different splitters (8, 16 & 32) between 1st & 2nd-stage SOA. The 2nd-stage QD-SOA with 8 & 16 splits have very high (P_{out} – *Penalty*) @ 10^{-7} BER, owing to its higher outputs and less penalties when operating at high input as compared to SOA#2. In summary, the 1st-stage SOA operating in small-signal gain region should have high gain, while the 2nd-stage SOA with moderate gain can be applied to save cost. But, this 2nd-stage SOA must well mitigate the pattern effect, and thus should have high saturation output since operating in saturation region. Finally, we compute the BERs of 3 SOAs based on theoretical & empirical equations and display together with experimental results. According to the BER plots versus SOA's input, the left side of minimum BER gets worse by OSNR degradation, while the right side gets worse by data pattern effect.

ACKNOWLEDGMENT

The authors are grateful to the 100th Anniversary Chulalongkorn University Fund for Doctoral Scholarship, The 90th Anniversary of Chulalongkorn University Fund (Ratchadaphiseksomphot Endowment Fund), and Overseas Research Experience Scholarship for Graduate Students from Graduate School Chulalongkorn University. The authors like to express appreciation to senior researchers and senior researcher engineer, especially Hiroyuki Sumimoto, for their help and advice at Photonic Network Laboratory, NICT.

REFERENCES

[1] T. Akiyama, M. Sugawara, and Y. Arakawa, "Quantum-dot semiconductor optical amplifiers," *Proc. IEEE*, vol. 95, pp. 1757–1766, 2007.

[2] G. Contestabile, A. Maruta, S. Sekiguchi, K. Morito, M. Sugawara, and K. Kitayama, "All-optical signal processing using QD-SOA," in *Proc. OECC Tech. Dig.*, 2010, pp. 200–201.

[3] D. Wang *et al.*, "Multifunctional all-optical signal processing scheme for simultaneous multichannel WDM multicast and XOR logic gates based on FWM in QD-SOA," in *Proc. Opt. Fiber Commun. Conf. Exhib.*, 2015, pp. 1–3.

[4] S. Sygletos *et al.*, "A wavelength conversion scheme based on a quantum-dot semiconductor optical amplifier and a delay interferometer," in *Proc. 10th Anniversary Int. Conf. Transparent Opt. Netw.*, 2008, pp. 149–152.

[5] G. Contestabile, Y. Yoshida, A. Maruta, and K. Kitayama, "Coherent wavelength conversion in a quantum dot SOA," *IEEE Photon. Technol. Lett.*, vol. 25, no. 9, pp. 791–794, May 2013.

[6] T. Ohtsuki, T. Yatsu, and M. Matsuura, "Regenerative wavelength conversion of PAM-4 signals using XGM with blue-shift filtering in a QD-SOA," in *Proc. Conf. Lasers Electro-Opt. Pacific Rim*, 2017, pp. 1–3.

[7] T. Ohtsuki and M. Matsuura, "Wavelength conversion of 25-Gbit/s PAM-4 signals using a quantum-dot SOA," *IEEE Photon. Technol. Lett.*, vol. 30, no. 5, pp. 459–462, Mar. 2018.

[8] B. Boriboon, D. Worasucheep, A. Matsumoto, K. Akahane, N. Yamamoto, and N. Wada, "Characteristics-improvement of QD semiconductor optical amplifier using rapid-thermal annealing process," in *Proc. Opt. Compon. Mater. XV*, vol. 10528, 2018, pp. 1–6.

[9] B. Boriboon, D. Worasucheep, A. Matsumoto, K. Akahane, N. Yamamoto, and N. Wada, "Optimized design of QD-LD toward QD-SOA to achieve 35-dB maximum chip gain with 400-mA injected current," *Opt. Commun.*, vol. 475, 2020, Art. no. 126238.

[10] K. Akahane, N. Yamamoto, S. Gozu, A. Ueta, N. Ohtani, and M. Tsuchiya, "Highly-ordered and highly-stacked (150-layers) quantum dots," in *Proc. Int. Conf. Indium Phosphide Related Mater. Conf. Proc.*, 2006, pp. 192–196.

[11] K. Akahane, N. Yamamoto, and T. Kawanishi, "Highly stacked quantum dot lasers fabricated by a strain-compensation technique," in *Proc. IEEE Photonic Soc. 24th Annu. Meeting*, 2011, pp. 163–164.

[12] S. Lange, Y. Yoshida, G. Contestabile, and K. Kitayama, "Phase transparent amplification of 40 Gbps 16 QAM signals using a QD-SOA," in *Proc. 18th Optoelectron. Commun. Conf. 2013 Int. Conf. Photon. Switching*, 2013, pp. 1–2.

[13] N. Yasuoka *et al.*, "Polarization-insensitive quantum dot semiconductor optical amplifiers using strain-controlled columnar quantum dots," *J. Lightw. Technol.*, vol. 30, pp. 68–75, 2012.

[14] *40-Gigabit-Capable Passive Optical Networks (NG-PON2): General Requirements*, ITU Telecommunications Standardization, ITU-T G.989.1, 2013.

[15] R. Bonk, H. Schmuck, W. Poehlmann, and T. Pfeiffer, "Beneficial OLT transmitter and receiver concepts for NG-PON2 using semiconductor optical amplifiers," *IEEE/OSA J. Opt. Commun. Netw.*, vol. 7, pp. A467–A473, 2015.

[16] N. A. Idris *et al.*, "A WDM/TDM access network based on broad T-Band wavelength resource using quantum dot semiconductor devices," *IEEE Photon. J.*, vol. 8, no. 1, Feb. 2016, Art. no. 7901510.

[17] R. Bonk *et al.*, "1.3/1.5 μm QD-SOAs for WDM/TDM GPON with extended reach and large upstream/downstream dynamic range," in *Proc. Conf. Opt. Fiber Commun.*, 2009, pp. 1–3.

[18] R. Bonk, H. Schmuck, B. Deppisch, W. Poehlmann, and T. Pfeiffer, "Wavelength-transparent long-reach-high-split TWsDM-PON utilized by a non-gated parallel cascade of linear SOAs," in *Proc. Eur. Conf. Opt. Commun.*, 2014, pp. 1–3.

[19] S. Shimizu and S. Shinada, "1024-way split, 70-km PAM4 transmission for PON uplink using cascaded SOAs and Volterra nonlinear equalization," in *Proc. OSA Adv. Photon. Congr. (AP) (IPR, NP, NOMA, Netw., PVLED, PSC, SPPCom, SOF)*, Washington, DC, USA, 2020, pp. 1–2.

[20] S. Liu *et al.*, "Cascaded performance of quantum dot semiconductor optical amplifier in a recirculating loop," in *Proc. Conf. Lasers Electro-Opt. Quantum Electron. Laser Sci. Conf.*, 2006, pp. 1–2.

[21] *40-Gigabit-Capable Passive Optical Networks 2 (NG-PON2): Physical Media Dependent (PMD) Layer Specification*, ITU Telecommunications Standardization, ITU-T G.989.2, 2019.

[22] S. Liu *et al.*, "High efficiency, high gain and high saturation output power quantum dot SOAs grown on Si and applications," in *Proc. Opt. Fiber Commun. Conf. Exhib.*, 2020, pp. 1–3.

[23] M. J. Connelly, "Structures," in *Semiconductor Optical Amplifiers*, MA, Boston, USA: Springer, 2002, pp. 21–41.

[24] THORLABS, *C-Band Semiconductor Optical Amplifier SOA1013S*, 19462-S01, Rev B datasheet, Jan. 2013.

[25] THORLABS, *C-Band Semiconductor Optical Amplifier*, Non-linear SOA1117S, 19463-S01, Rev B datasheet, May 2016.

[26] G. P. Agrawal, "Optical amplifiers," in *Fiber-Optic Communication Systems*, Canada: Wiley-Interscience, 2002, ch. 6, pp. 226–278.

[27] D. M. Baney, P. Gallion, and R. S. Tucker, "Theory and measurement techniques for the noise figure of optical amplifiers," *Opt. Fiber Technol.*, vol. 6, pp. 122–154, 2000.

[28] YOKOGAWA, *AQ6375 Optical Spectrum Analyzer*, IM 735305-01E datasheet, Dec. 2007.

[29] J. Mork, M. L. Nielsen, and T. W. Berg, "The dynamics of semiconductor optical amplifiers: Modeling and applications," *Opt. Photon. News*, vol. 14, pp. 42–48, 2003.

[30] H. Schmeckebier, "Introduction to semiconductor optical amplifiers (SOAs)," in *Quantum-Dot-Based Semiconductor Optical Amplifiers for O-Band Optical Communication*, Cham, Switzerland: Springer, 2017, ch. 2, pp. 13–34.

[31] G. Contestabile, A. Maruta, and K. Kitayama, "Gain dynamics in quantum-dot semiconductor optical amplifiers at 1550 nm," *IEEE Photon. Technol. Lett.*, vol. 22, no. 13, pp. 987–989, Jul. 2010.

[32] Y. Ben-Ezra, M. Haridim, and B. I. Lembrikov, "Theoretical analysis of gain-recovery time and chirp in QD-SOA," *IEEE Photon. Technol. Lett.*, vol. 17, no. 9, pp. 1803–1805, Sep. 2005.
[33] M. Matsuura, H. Ohta, and R. Seki, "Dynamic frequency chirp properties of QD-SOAs," in *Proc. Opt. Fiber Commun. Conf. Exhib.*, 2015, pp. 1–3.
[34] T. Watanabe, N. Sakaida, H. Yasaka, F. Kano, and M. Koga, "Transmission performance of chirp-controlled signal by using semiconductor optical amplifier," *J. Lightw. Technol.*, vol. 18, no. 8, pp. 1069–1077, Aug. 2000.
[35] W. Freude *et al.*, "Linear and nonlinear semiconductor optical amplifiers," in *Proc. 12th Int. Conf. Transparent Opt. Netw.*, 2010, pp. 1–4.
[36] P. N. Goki, M. Imran, F. Fresi, F. Cavaliere, and L. Potì, "Lossless ROADM by exploiting low gain SOAs in fronthaul network," in *Proc. 24th Optoelectron. Commun. Conf. Int. Conf. Photon. Switching Comput.*, 2019, pp. 1–3.
[37] R. Bonk *et al.*, "The input power dynamic range of a semiconductor optical amplifier and its relevance for access network applications," *IEEE Photon. J.*, vol. 3, no. 6, pp. 1039–1053, Dec. 2011.
[38] M. L. Davenport, S. Skendzic, N. Volet, and J. E. Bowers, "Heterogeneous silicon/InP semiconductor optical amplifiers with high gain and high saturation power," in *Proc. Conf. Lasers Electro-Opt.*, 2016, pp. 1–2.
[39] OPTOQUEST, *Angle Tunable Type Wavelength Tunable Filter Module*, March 2015.
[40] SHF Communication Technologies AG, SHF 810 - v002 datasheet, Feb. 2007.